Literature Report

Reporter: zhou wei

Date: 2020-02-13

JACS
JOURNAL OF THE AMERICAN CHEMICAL SOCIETY
pubs.acs.org/JACS
Article

NIR Scaffold Bearing Three Handles for Biocompatible Sequential Click Installation of Multiple Functional Arms

Yuqi Wang, Jianhui Weng, Jianguo Lin, Deju Ye, and Yan Zhang*

南京大学化学化工学院

光化学生物学。包括光诱导生物正交反应的开发，基于有机光反应构建解析活细胞等生物体系内复杂分子事件的“分子侦探”，基于光反应对生物体系的时空分辨调控等。

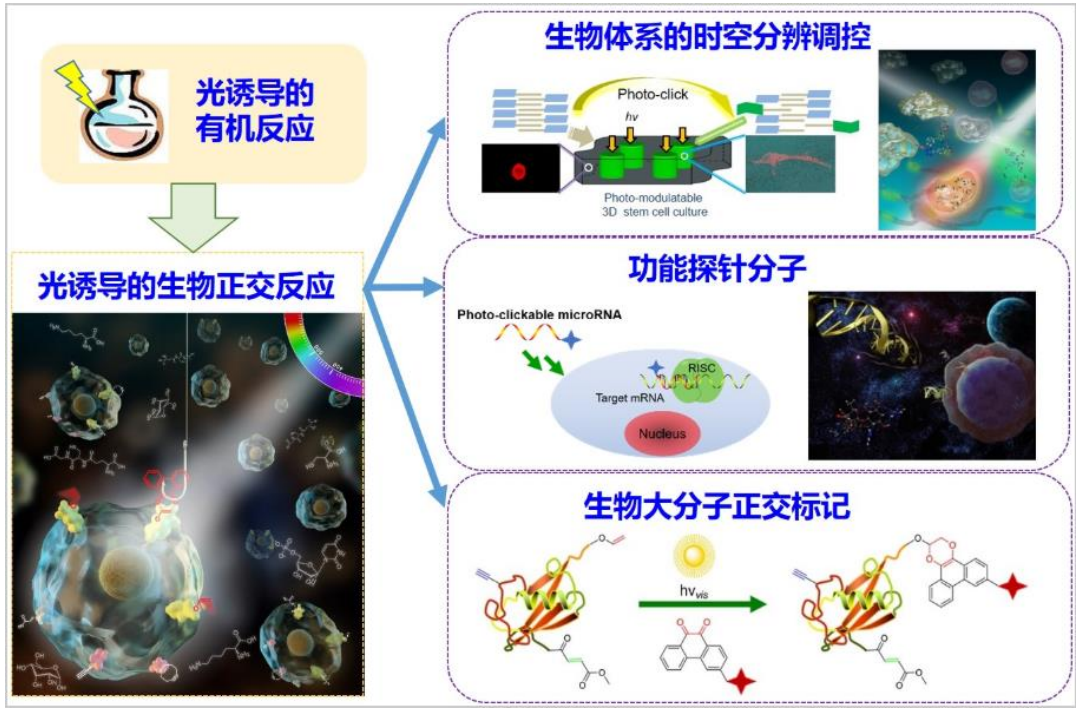

JACS
JOURNAL OF THE AMERICAN CHEMICAL SOCIETY

Communication

Cite This: J. Am. Chem. Soc. 2018, 140, 14542−14546

pubs.acs.org/JACS

Visible Light-Initiated Bioorthogonal Photoclick Cycloaddition

Jinbo Li,[†,§] Hao Kong,[†,§] Lei Huang,[†,§] Bo Cheng,[‡] Ke Qin,[‡] Mengmeng Zheng,[†] Zheng Yan,[†] and Yan Zhang*[,†]

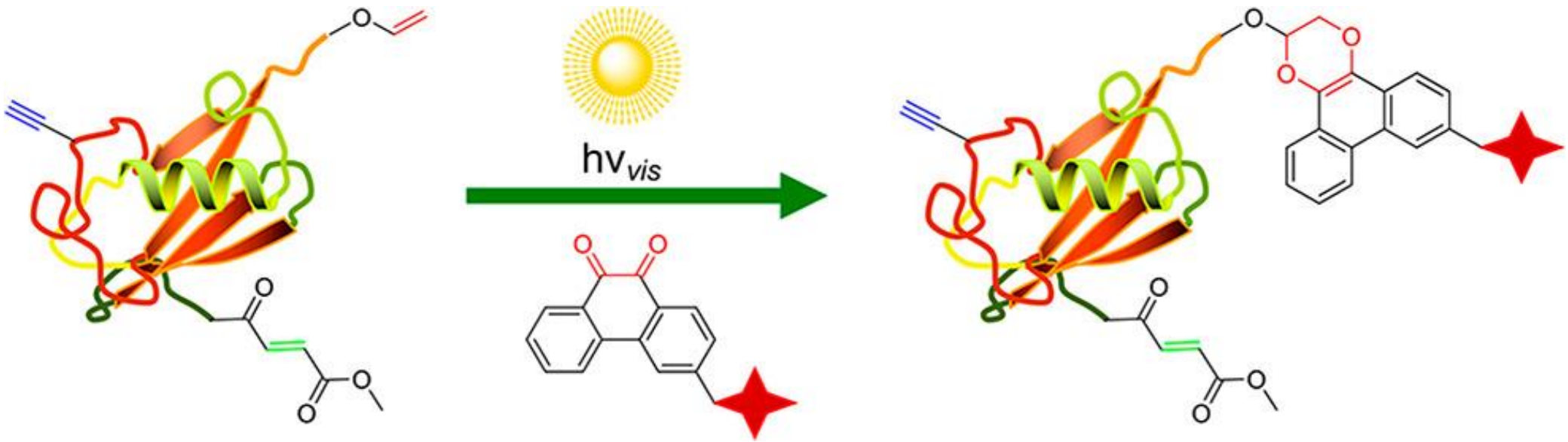

JACS
JOURNAL OF THE AMERICAN CHEMICAL SOCIETY

Article

pubs.acs.org/JACS

Photoclickable MicroRNA for the Intracellular Target Identification of MicroRNAs

Jinbo Li,[†,‡] Lei Huang,[†] Xiao Xiao,[†] Yingjie Chen,[†] Xingxing Wang,[†] Zhengquan Zhou,[†] Chenyu Zhang,[*,‡] and Yan Zhang[*,†,‡]

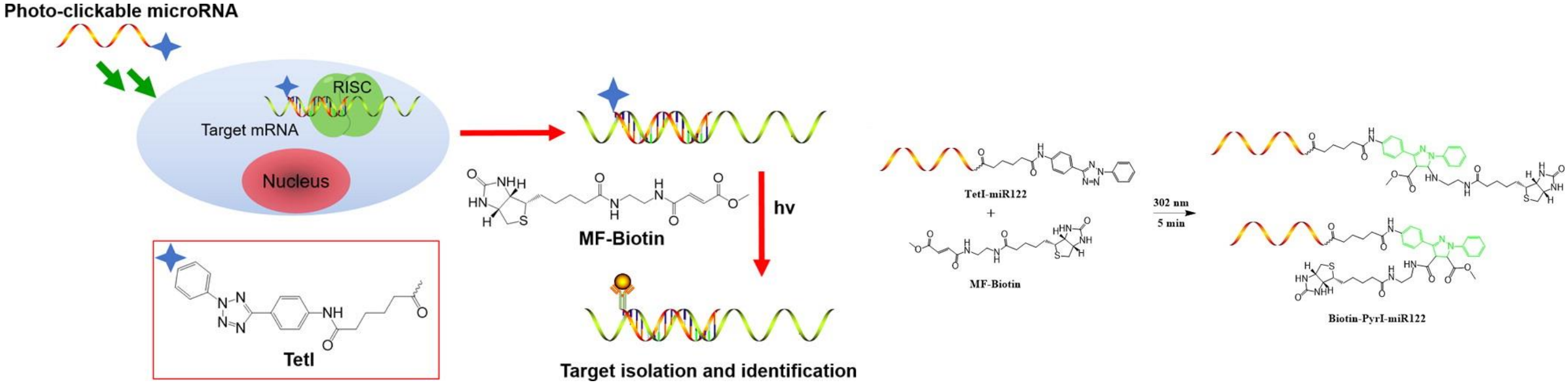

设计思路

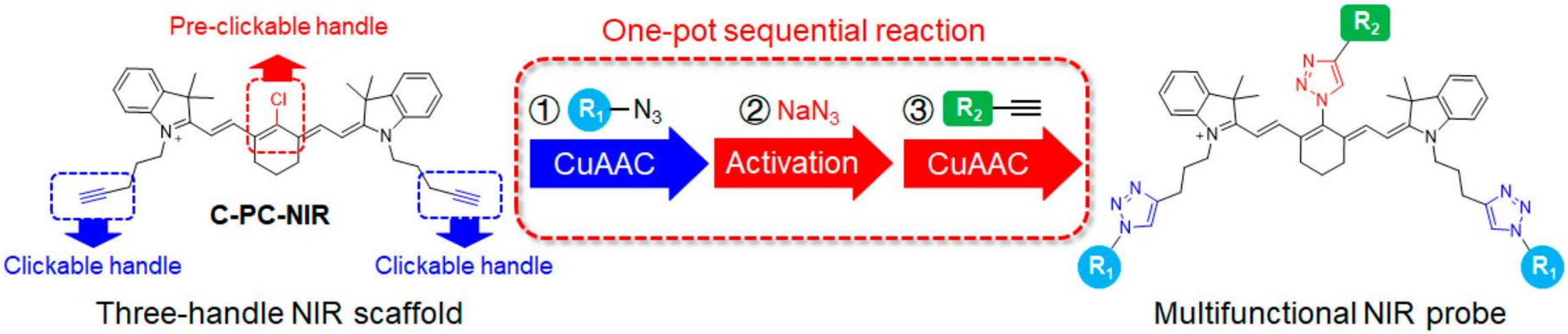
Pre-clickable handle
One-pot sequential reaction
Cl
C-PC-NIR
① R1–N3
② NaN3
③ R2
CuAAC
Activation
CuAAC
Clickable handle
Clickable handle
R2
R1
R1
Three-handle NIR scaffold
Multifunctional NIR probe

R_1, R_2 =

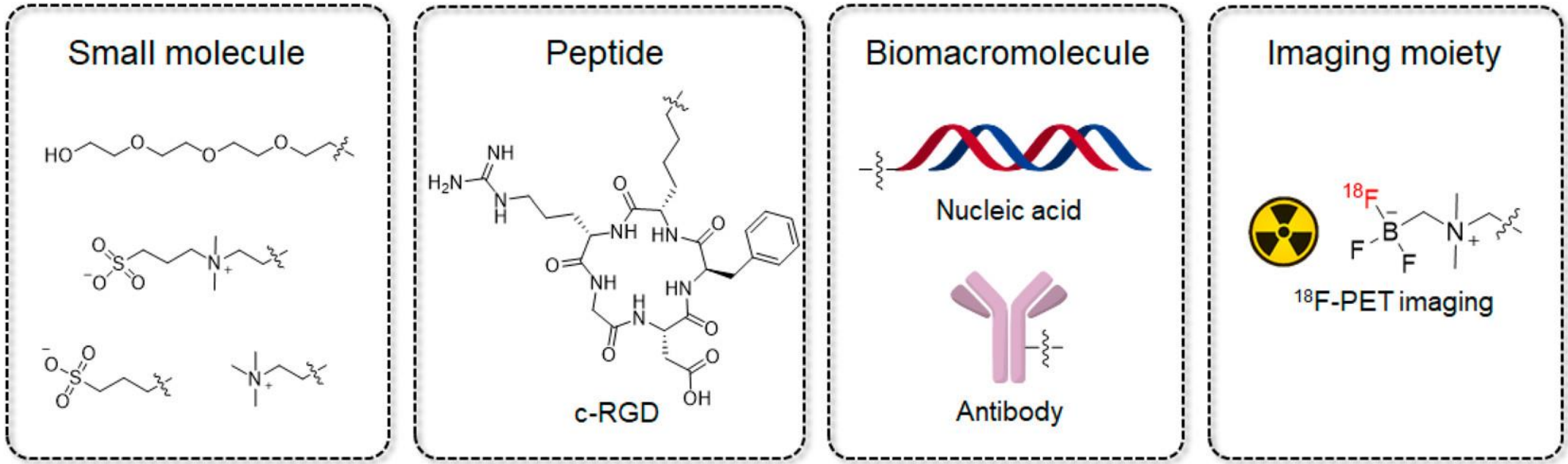
Small molecule
HO
Peptide
c-RGD
Biomacromolecule
Nucleic acid
Antibody
Imaging moiety
18F
18F-PET imaging

连接基团电荷对骨架的影响

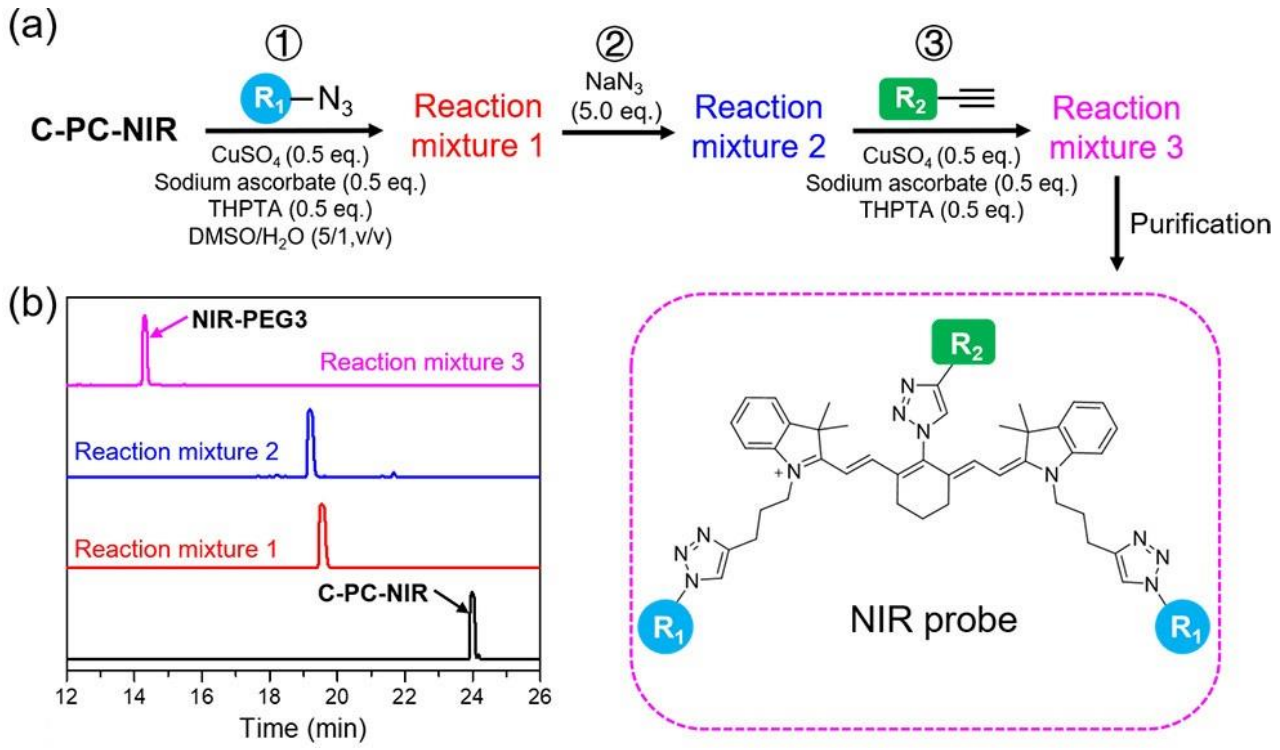

(c)

Entry	1	2	3	4
R_1	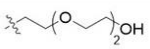		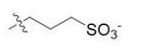	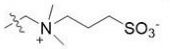
R_2	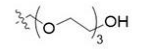		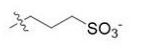	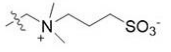
Product	NIR-PEG3	NIR-PC	NIR-NC	NIR-ZW
λ_{ex} (nm)	790	795	790	795
λ_{em} (nm)	805	809	805	811
Stokes shift (nm)	15	14	15	16
ε ($M^{-1}cm^{-1}$)	186600	149400	161600	132000
QY (%)[a]	3.22	1.84	3.16	2.36
Photothermal conversion efficiency (%)[b]	28.6	28.3	16.4	30.2
$^1O_2$ quantum yield[c]	0.032	0.040	0.022	0.023
Yield (%)	91	92	86	83

Figure 1. (c) Structure of the positively charged arms, negatively charged arms, and zwitterionic arms installed to the NIR scaffold and the maximum excitation wavelength (λ_{ex}), maximum emission wavelength (λ_{em}), Stokes shift, extinction coefficient (ε), absolute fluorescence quantum yield (QY), photothermal conversion efficiency, ^{1}O2 quantum yield, and isolated yields of the corresponding products. Notes: a The absolute fluorescence quantum yield (QY) is defined as QY = PN_{em} /PN_{abs}, where PN_{em} and PN_{abs} are the number of emitted and absorbed photons by fluorescence probes. Excitation wavelengths were set to 795 nm for NIR-PC and NIR-ZW and 790 nm for NIR-PEG3 and NIR-NC. All the QY were measured in PBS (1×, pH = 7.4). concentration of each probe was 1 μM b The photothermal conversion efficiency were measured in PBS (1×, pH = 7.4). The concentration of each probe was 10 μM. The photothermal conversion efficiency of ICG was measured to be 19.2% under the same conditions. c The ^{1}O2 quantum yield of each compound were measured in PBS (1×, pH = 7.4). The concentration of each probe was 2 μM. ICG was used as reference compound whose ^{1}O2 quantum yield was reported to be 0.008 in aqueous solution.

连接基团电荷对骨架的影响

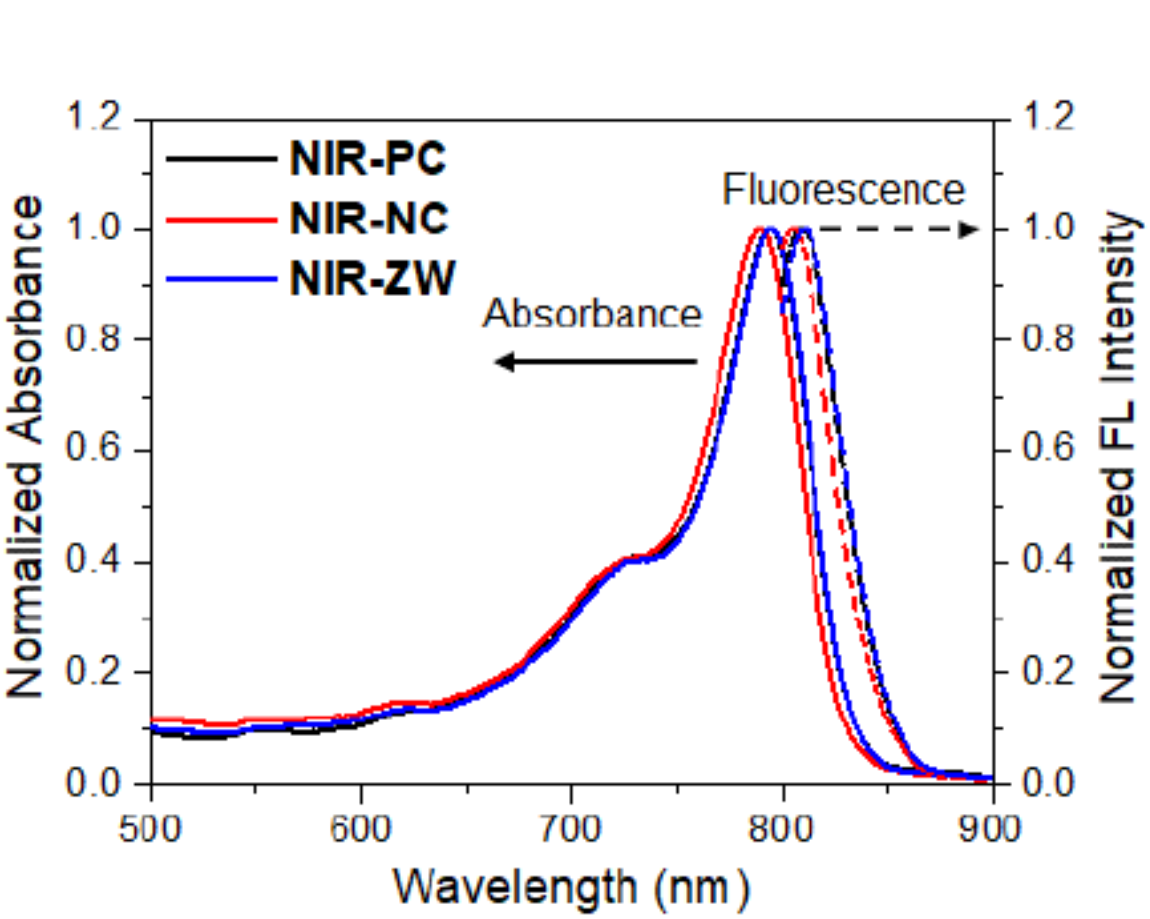

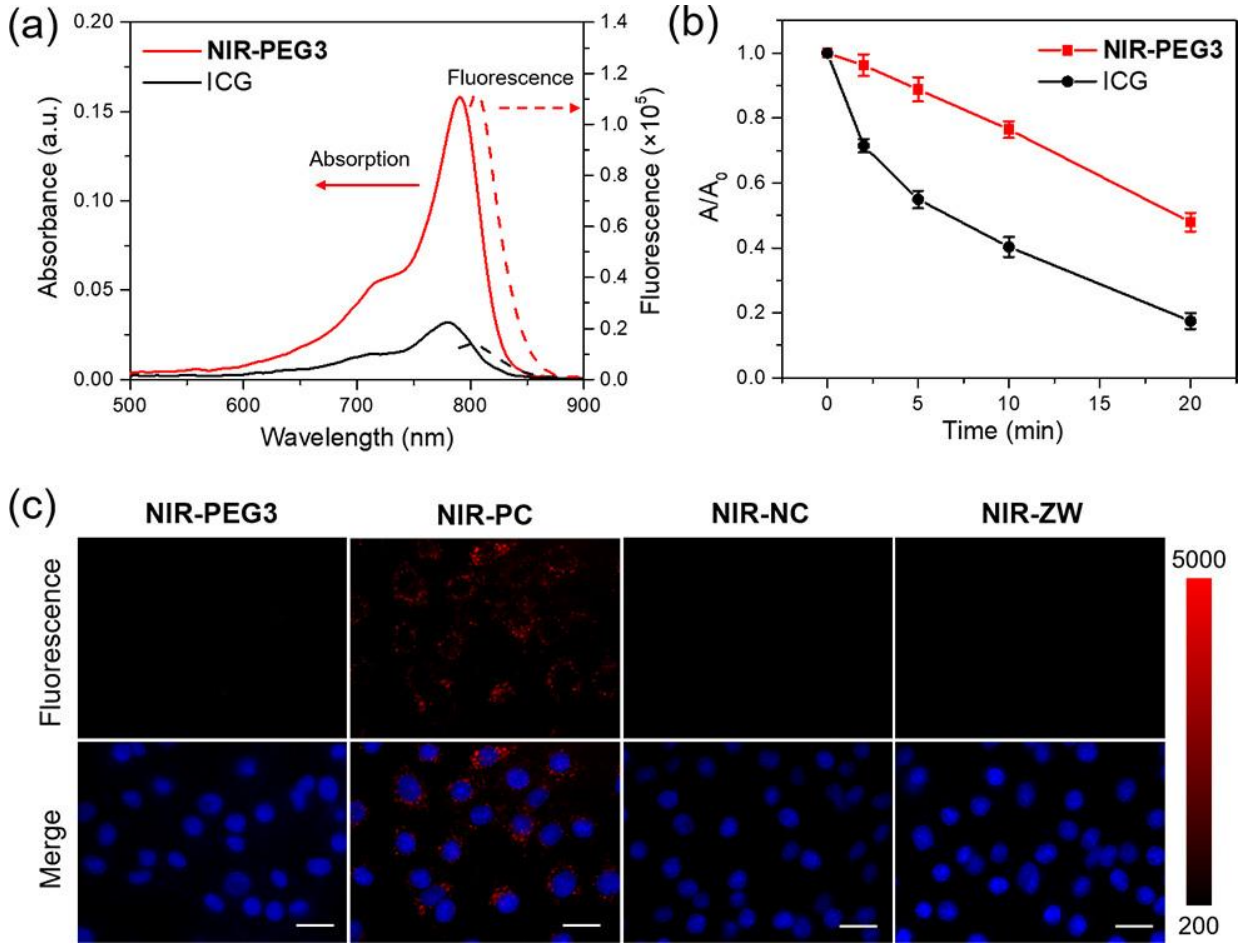

Figure 2. (a) Fluorescence spectra (dashed line) and absorption spectra (solid line) of NIR-PEG3 and ICG in 1× PBS buffer (concentration: 1 μM). For NIR-PEG3, Ex = 790 nm. For ICG, Ex = 780 nm. (b) Photostability analysis of NIR-PEG3 (red) and ICG (black) (both at 10 μM in PBS) under laser irradiation (785 nm, 40 mW) for different times. A/A0 represents the ratio of absorbance before and after irradiation for the corresponding time. Mean value ± SD (n = 3) was exhibited. (c) Fluorescence imaging of HeLa cells incubated with NIR-PEG3, NIR-PC, NIR-NC, and NIR-ZW (5 μM) for 24 h. Cellular nuclei were stained with Hoechst 33342 (concentration: 0.1 μg/mL). For Hoechst 33342, Ex = 365 ± 25 nm, and Em = 440 ± 20 nm. For NIR-PEG3, NIR-PC, NIR-NC, or NIR-ZW, Ex = 775 ± 25 nm, and Em = 845 ± 25 nm. Scale bar: 20 μm.

实现精准靶标个数与位置的连接及其影响

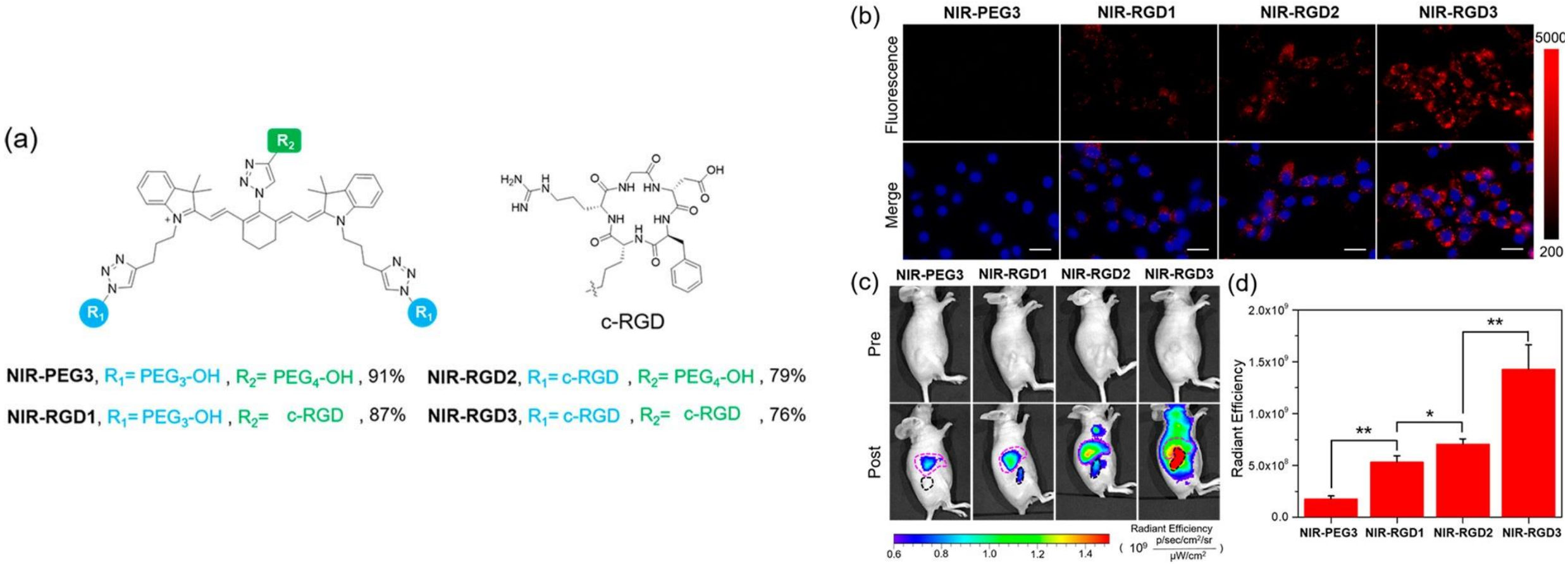

Figure 3. (a) Chemical structure of NIR fluorescent probes without c- RGD group (NIR-PEG3), or with one c-RGD group (NIR-RGD1), two c-RGD groups (NIR-RGD2), or three c-RGD groups (NIRRGD3). (b) U87MG cells incubated with NIR-PEG3, NIR-RGD1, NIR-RGD2, or NIR-RGD3 (5 μM) for 24 h under fluorescence microscopy. Nucleus staining by Hoechst 33342 (0.1 μg/mL) and acquired with Ex = 365 ± 25 nm, Em = 440 ± 20 nm. For NIR-PEG3, NIR-RGD1, NIR-RGD2, or NIR-RGD3, Ex = 775 ± 25 nm, Em = 845 ± 25 nm. Scale bar: 20 μm. (c) U87MG tumor xenograft mice before (Pre) treatment and 6 h after receiving iv injections of NIRPEG3, NIR-RGD1, NIR-RGD2, or NIR-RGD3 (25 μM, 200 μL) (Post). The locations of tumors or livers in each image are indicated by black circles and rose red circles, respectively. (d) Quantification of the radiant efficiency in U87MG tumors after iv injection of NIRPEG3, NIR-RGD1, NIR-RGD2, or NIR-RGD3 (5 nmol) for 6 h. Mean value ± SD (n = 3) was exhibited. *$p < 0.05$, **$p < 0.01$.

实现核酸、抗体的标记成像

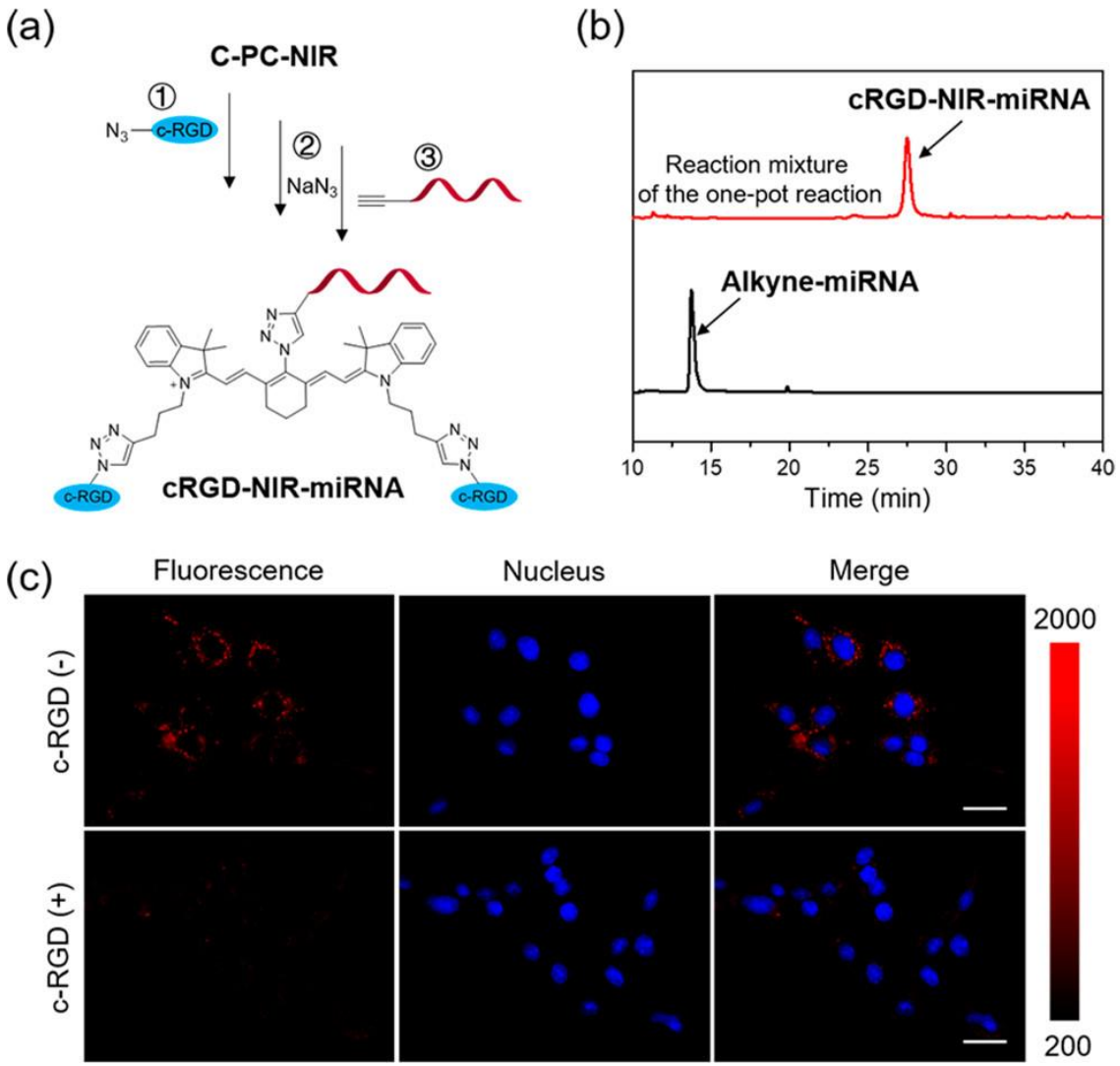

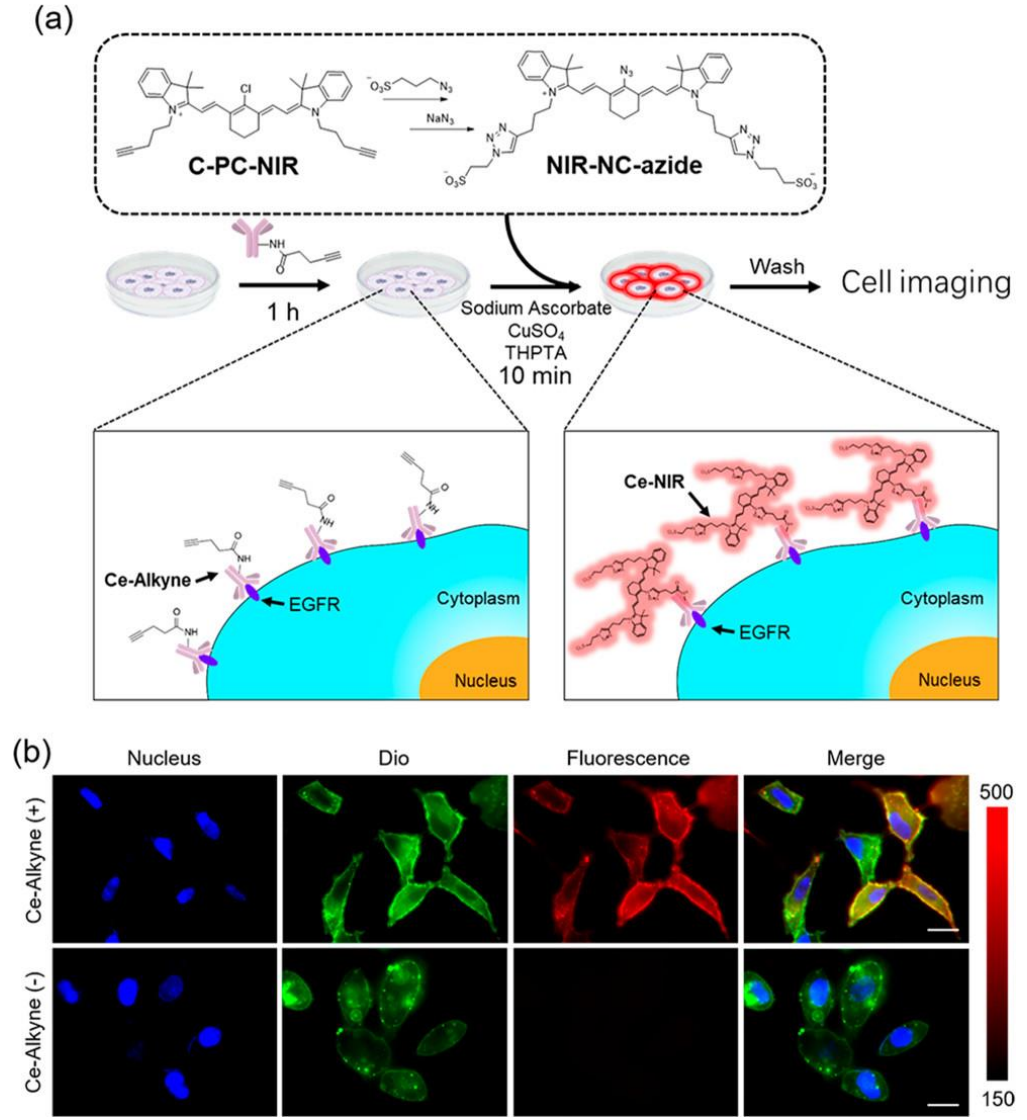

实现荧光与PET成像联用

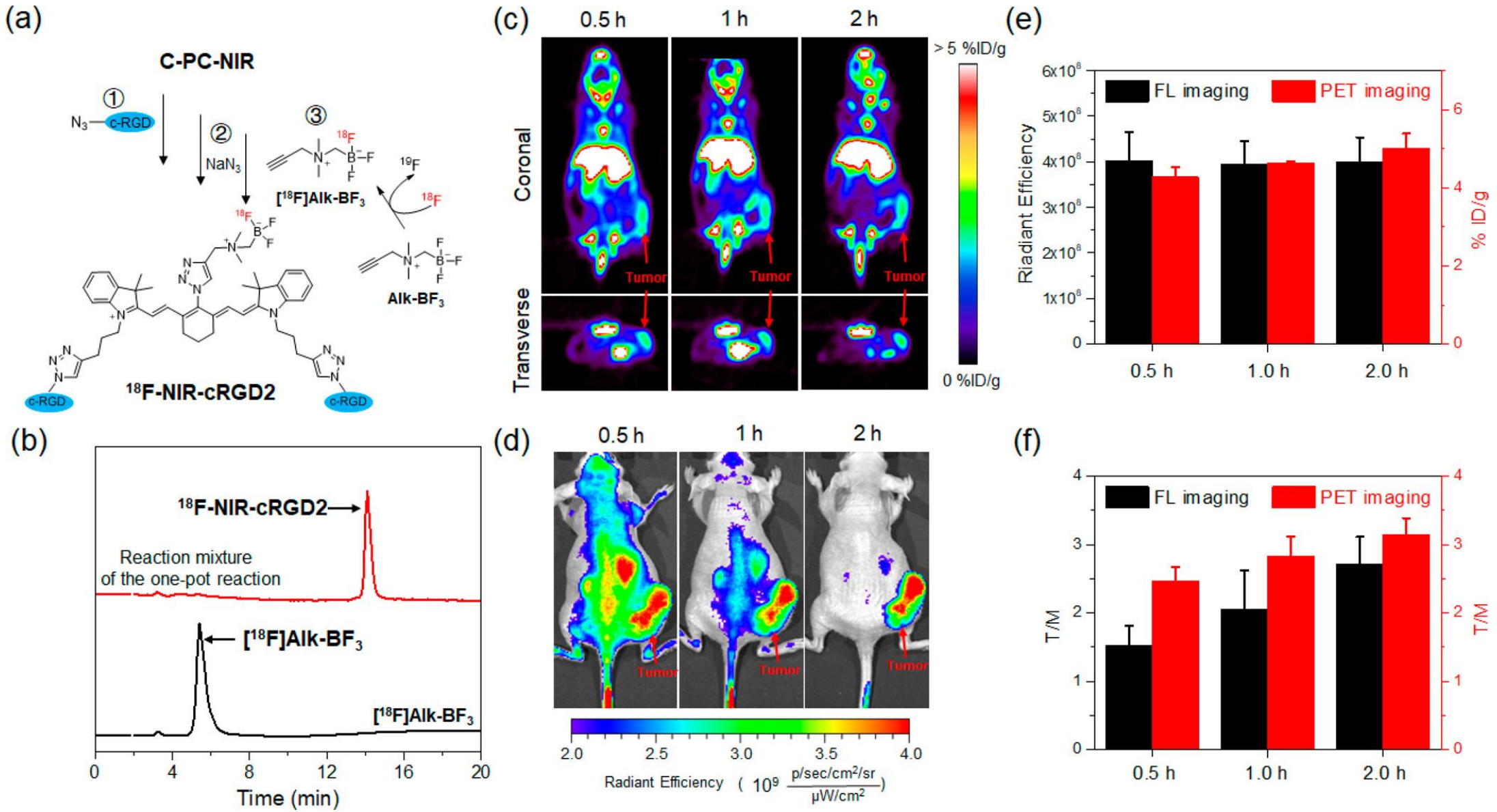

Thanks !